Kinetics of Reduction of High Redox Potential Ferredoxins by the Semiquinones of *Clostridium pasteurianum* Flavodoxin and Exogenous Flavin Mononucleotide. Electrostatic and Redox Potential Effects†

C. T. Przysiecki, G. Cheddar, T. E. Meyer, G. Tollin, and M. A. Cusanovich*
Department of Biochemistry, University of Arizona, Tucson, Arizona 85721
Received February 25, 1985

ABSTRACT: We have measured the ionic strength dependence of the rate constants for the electron-transfer reactions of flavin mononucleotide (FMN) and flavodoxin semiquinones with 10 high redox potential ferredoxins (HiPIP's). The rate constants were extrapolated to infinite ionic strength by using a theoretical model of electrostatic interactions developed in our laboratory. In all cases, the sign of the electrostatic interaction was the same as the protein net charge, but the magnitudes were much smaller. The results are consistent with a model in which the electrical charges are approximately uniformly distributed over the HiPIP surface and in which there are both short- and long-range electrostatic interactions. An electrostatic field calculation for *Chromatium vinosum* HiPIP is consistent with this. The presumed site of electron transfer includes that region of the protein surface to which the iron–sulfur cluster is nearest and appears to be relatively hydrophobic. The principal short-range electrostatic interaction would involve the negative charge on the iron–sulfur cluster. For some net negatively charged proteins, this effect is magnified, and for net positively charged HiPIP's, it is counterbalanced. The rate constants extrapolated to infinite ionic strength can be correlated with redox potential differences between the reactants, as has previously been shown for cytochrome–flavin semiquinone reactions. Both electrostatic and redox potential effects are magnified for the flavodoxin semiquinone as compared to the FMN semiquinone–HiPIP reactions. This was also observed previously for the flavin semiquinone–cytochrome reactions. The present work provides further support for the universal nature of those factors (redox potential differences and steric and electrostatic interactions) which we have found to govern the rates of redox protein electron-transfer reactions and which therefore determine biological specificity.

Oxidation–reduction reactions between various soluble, nonphysiologically interacting redox proteins have been studied by several laboratories as model systems for developing an understanding of the mechanisms of biologically important electron-transfer reactions [cf. Wherland & Pecht (1978), Mizrahi & Cusanovich (1980), Aprahamian & Feinberg (1981), Geren & Millett (1981), Simondsen et al. (1982), and Augustin et al. (1984)]. These investigations have involved flavin, heme, copper, or iron–sulfur containing redox proteins and, in general, have stressed the influence of electrostatic interactions on the rate constant of the electron-transfer reaction. It is to be expected that other factors would also affect protein–protein electron-transfer processes, e.g., steric effects, relative exposure of the redox groups, hydrophobic interactions, and the redox potential differences between donor and acceptor, but these influences have been difficult to demonstrate and to quantitate. In part, such difficulties have arisen from the dominant role of electrostatic interactions in many protein–protein redox reactions, from the limited redox potential range displayed by many classes of electron-transfer proteins, and from the lack of three-dimensional structural information for at least one member of the protein classes being investigated.

In recent studies from this laboratory of the reduction kinetics of a large number of structurally homologous *c*-type cytochromes by exogenous flavin semiquinones and by the semiquinone redox state of *Clostridium pasteurianum* flavodoxin (an FMN-containing flavoprotein), we were able to quantitate electrostatic effects, redox potential, and steric effects (Meyer et al., 1983, 1984; Tollin et al., 1984). This was accomplished by extrapolating the second-order rate constants to infinite ionic strength (k_∞) using the electrostatic equation of Watkins (1984) in order to compensate for charge interactions and by fitting the calculated k_∞ values to curves generated from semiempirical (Marcus, 1968) and theoretical (Hopfield, 1974) free energy equations which relate the second-order rate constant to the difference in redox potential between the reactants (ΔE). This approach was first shown to work quite well for free flavin semiquinone reduction of these cytochromes (Meyer et al., 1984). Deviations from the free energy relationships were interpreted in terms of steric effects resulting from differences between the cytochrome *c* three-dimensional structures. By comparing the flavodoxin semiquinone reduction kinetic parameters with those obtained upon free FMN semiquinone reduction of the same group of cytochromes, it was found that, although the results were qualitatively similar, the magnitudes of the effects of electrostatics, redox potential, and steric interactions were much larger for the flavodoxin reactions, suggesting that these factors were involved in the establishment of biological specificity between redox chromophores in protein–protein reactions (Tollin et al., 1984).

In order to examine whether or not the results of the cytochrome–flavodoxin study can be generalized to other classes of redox proteins, we have investigated the reduction of high-potential 4Fe–4S ferredoxins (HiPIP's) by free FMN and flavodoxin semiquinones. The availability of a three-dimensional structure of one HiPIP, from *Chromatium vinosum* (Carter, 1977), knowledge of the amino acid sequences of other examples (Tedro et al., 1981), and a large, thermodynamically favorable redox potential range (+50 to +450 mV; Meyer et

† This work was supported in part by grants from the National Institutes of Health [AM15057 (G.T.) and GM21277 (M.A.C.)].

0006-2960/85/0424-5647$01.50/0

al., 1983) provide this class of Fe–S proteins with advantageous properties. In addition, the net charge of different HiPIP examples varies from slightly basic to strongly acidic (Bartsch, 1978), with the presumed site of electron transfer being largely hydrophobic in nature (Mizrahi & Cusanovich, 1980; Aprahamian & Feinberg, 1981), in contrast to the strong positive charge at the site of electron transfer for mitochondrial cytochrome *c* reactions.

Despite the quite different chemical structures and solvent exposures of the redox chromophores in HiPIP and cytochrome *c*, the present work demonstrates that similar results can be obtained with these two classes of protein for the influence of redox potential and electrostatic interactions on the reactions of flavodoxin and FMN semiquinones. Furthermore, as was found with the cytochromes, the magnitudes of the electrostatic and redox potential effects on the flavodoxin reaction with HiPIP are larger than for the FMN reaction. This provides further support for the universal importance of these factors in determining biological specificity for protein–protein electron-transfer reactions (Tollin et al., 1984). The results also suggest that contributions from both long-range and localized charge interactions can influence the electrostatics of these redox reactions, as was previously concluded from the cytochrome kinetics (Meyer et al., 1984; Tollin et al., 1984).

Materials and Methods

HiPIP's from the various sources were completely purified following the general procedure described by Bartsch (1978), and purity indexes (A_{280}/A_{390}) were the same as published values. $\Delta\epsilon_{530nm}$ = 7.3 mM^{-1} cm^{-1} was used to calculate the concentration of all HiPIP's. *C. pasteurianum* flavodoxin was obtained as described previously (Simondsen et al., 1982). The oxidation of HiPIP's has been described (Przysiecki et al., 1984) as has the purification of FMN (Nagy et al., 1982). The procedure for the preparation of flavodoxin semiquinone and anaerobic solutions of the reactants at different ionic strengths is described elsewhere (Simondsen et al., 1982). Buffers for the FMN–HiPIP reactions contained 10 mM potassium phosphate, 5 mM ethylenediaminetetraacetic acid (EDTA), pH 7.0, and the appropriate amounts of KCl to give the indicated ionic strengths. Solutions containing FMN were prepared immediately prior to use and contained approximately 40 μM oxidized FMN. The procedure for degassing solutions for free FMN experiments has been described (Cusanovich & Tollin, 1980). The stopped-flow apparatus used for the flavodoxin–HiPIP reactions (Jung & Tollin, 1981) and the laser flash photolysis apparatus used for the free FMN–HiPIP reactions (Simondsen & Tollin, 1983) have also been described previously.

The in situ photoreduction of flavodoxin semiquinone by the 5-deazariboflavin–EDTA system also generates fully reduced flavodoxin. Although the exact amount of this species produced is unknown under the present experimental conditions, the small decrease in oxidized HiPIP concentration resulting from these additional reduced flavodoxin equivalents (fully reduced flavodoxin reacts with HiPIP within the mixing time of the stopped-flow apparatus) was corrected for by subtracting the initial amount of oxidized flavodoxin from the initial HiPIP concentration (i.e., this assumes that all of the oxidized flavodoxin is converted to the fully reduced oxidation state). Since the HiPIP concentration is considerably larger than that of the flavodoxin (pseudo-first-order conditions), this correction is relatively small. Data acquisition and analysis for the HiPIP–free FMN reactions were as previously described for other free flavosemiquinone reactions (Przysiecki et al., 1984) and involved measuring the observed rate constant at five

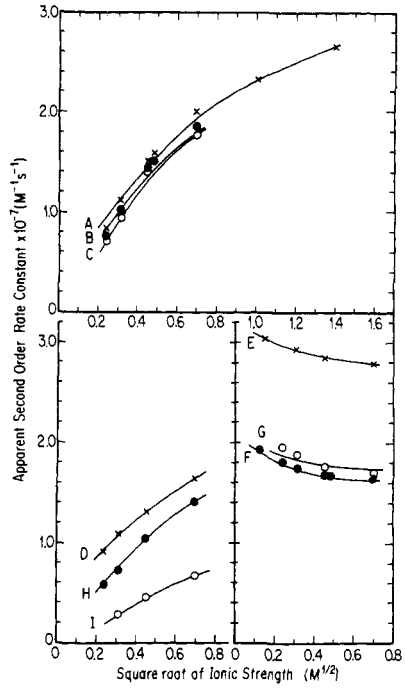

FIGURE 1: Plots of the apparent second-order rate constants for FMN semiquinone oxidation by HiPIP vs. the square root of the ionic strength. Solid lines represent calculated theoretical values for the data obtained by using eq 1 (see text for details). Curves for different HiPIP's labeled as in Table I.

HiPIP concentrations (typically a 10-fold range) for each ionic strength studied. We estimate that the precision in the rate constant determinations for both the flavodoxin and the FMN systems was ±15%.

Results and Discussion

Plots of the apparent second-order rate constants vs. the square root of the ionic strength for the reaction of nine different HiPIP's with FMN semiquinone are shown in Figure 1. The solid lines in Figure 1 were obtained by using the electrostatic equation (eq 1 below) for bimolecular reactions

$$\ln k(I) = \ln k_\infty - V_{ii}X(I) \qquad (1)$$

of Watkins (1984). This equation has previously been successfully used to fit the kinetic data for the analogous reaction systems involving FMN and flavodoxin semiquinones and various *c*-type cytochromes (Meyer et al., 1984; Tollin et al., 1984). Equation 1 treats the interaction domain of the reactants, FMN semiquinone and oxidized HiPIP, as parallel disks (of radius ρ) with discrete point charges (Z_1, Z_2) equal to the total charge in the localized region of interaction of the reactants, which results in an electrostatic potential energy (V_{ii}). In this equation, $k(I)$ is the observed rate constant at ionic strength I, k_∞ is the rate constant at infinite ionic strength, and V_{ii} is as defined above and equal to $\alpha Z_1 Z_2 R_{12} \rho^{-2} D_e^{-1}$ (ρ, Z_1, and Z_2 are as defined above, R_{12} is the distance between reactant chromophores in the transient complex leading to products, and D_e is the effective dielectric constant at the site of interaction) (Meyer et al., 1984; Watkins, 1984). $X(I)$ is an ionic strength dependent term containing the parameter κ [$X(I) = (1 + \kappa\rho)^{-1} \exp(-\kappa\rho)$]. The curves were calculated by using ρ = 4 Å, a value which is consistent with the size of FMN and which was found to give excellent fits. In similar studies with *c*-type cytochromes, ρ values of 4–5 Å were also found to be appropriate (Meyer et al., 1984). Given the value of ρ noted above, the experimental data were fitted to give a minimum least-squares error yielding

Table I: Effect of Ionic Strength on the Oxidation of FMN Semiquinone by HiPIP

HiPIP source	$E_{m,7}$ (V)	net charge[a]	no. of His residues	V_{ii} (kcal/mol)	ρ (Å)	Z_1[b]	$k_\infty \times 10^7$ (M^{-1} s^{-1})
C. vinosum	0.36	4–	1	+2.10	4.0	−0.9	3.0
C. gracile	0.35	6–	2	+2.37	4.0	−1.0	3.1
T. pfennigii	0.35	8–	4	+2.58	4.0	−1.1	3.0
T. roseopersicina	0.34	5–	3	+1.65	4.0	−0.7	2.3
Rps. gelatinosa	0.33	4+	1	−0.20	4.0	+0.1	2.7
Rsp. tenue 3761	0.30	3+	0	−0.29	4.0	+0.1	1.5
Rsp. tenue 2761	0.30	2+	0	−0.23	4.0	+0.1	1.7
E. vacuolata iso-1	0.26	4–	3	+2.46	4.0	−1.0	2.3
E. vacuolata iso-2	0.15	7–	2	+3.43	4.0	−1.4	1.4
E. halophila iso-1	0.12	11–	4	*c*	*c*	*c*	*c*

[a] Net charges were calculated from published amino acid sequences or from unpublished sequences (T. E. Meyer, unpublished observations). The 1– cluster charge of oxidized HiPIP is included. It was assumed that all histidines were unprotonated, but this is probably not the case [cf. Nettessheim et al. (1983)]. [b] Z_1, the apparent charge on HiPIP at its interaction site, was obtained from $V_{ii} = \propto Z_1 Z_2 R_{12} \rho^{-2} D_e^{-1}$, where $\propto$ = 128.47, Z_2 = −1.9 (charged FMN at pH 7), R_{12} = 8.0 Å [van der Waals radii (3.5 Å) plus distance of closest approach of the iron–sulfur cluster to the HiPIP surface (4.5 Å)], ρ is the radius of the site of interaction as given in the table, and D_e is the effective dielectric constant at the site of interaction (a value of 50 was used). See text for further discussion of the parameters. [c] Too slow to measure.

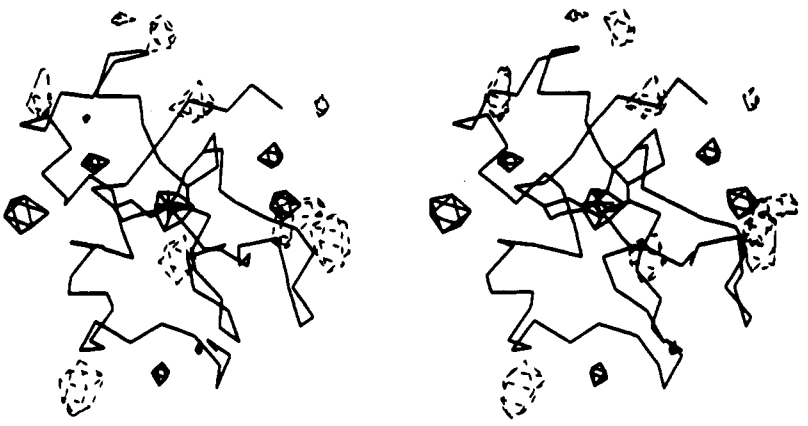

FIGURE 2: Stereoview of the calculated electrostatic fields for *Chromatium vinosum* HiPIP at the 2-kT energy level overlaid on the backbone structure. Dashed lines are regions of negative field, and solid lines are regions of positive field. Iron–sulfur cluster charge not included.

values for k_∞ and V_{ii}. These are summarized in Table I along with Z_1, the apparent charge on HiPIP at the site of interaction, which was calculated from V_{ii} by using the equation noted above, a charge of 1.9– on FMN semiquinone (Z_2), and an effective dielectric constant at the site of interaction (D_e) of 50. This same value for D_e was previously found to be appropriate for analysis of the interaction of FMN semiquinone and *c*-type cytochromes (Meyer et al., 1984) and is consistent with measurements of the surface dielectric constant of horse heart cytochrome *c*, which is an example of a small, globular water-soluble protein (Rees, 1980). R_{12}, the distance of closest approach of the two reactants, was taken as 8.0 Å, which is the van der Waals radii (3.5 Å) plus the distance of closest approach of the iron–sulfur cluster to the HiPIP surface (4.5 Å; Carter et al., 1974).

Application of the electrostatic equation of Wherland & Gray (1976) [$\ln k(I) = \ln k_\infty - 3.576[(1 + \kappa R_2)^{-1} \exp(-\kappa R_1) + (1 + \kappa R_1)^{-1} \exp(-\kappa R_2)] Z_1 Z_2 (R_1 + R_2)^{-1}$] yields fits of generally similar quality for the second-order rate constant vs. square root of ionic strength plots (Figure 1). However, this equation requires the use of full protein radii (R_1, R_2) and net protein charges (Z_1, Z_2) (Wherland & Gray, 1976) and thus presupposes that local charges are of no consequence. In our previous cytochrome–flavin semiquinone studies (Meyer et al., 1984; Tollin et al., 1984), we found examples which gave ionic strength effects opposite in sign to what were expected from the net protein charges. The Wherland–Gray treatment obviously cannot deal with such situations. Values of k_∞ were generally smaller when obtained from the Wherland–Grey equation as compared with those obtained by using eq 1, although they had approximately the same relative magnitudes. This occurred because at high ionic strength (>500 mM) the Wherland–Gray equation becomes independent of ionic strength (a consequence of the use of full protein radii) more quickly than does eq 1, which accurately describes the observed data up to 2 M ionic strength (Figure 1, curve A). In view of these limitations, the analyses below will be given in terms of eq 1, which more accurately models the experimental results.

The values of the charge at the interaction site on the various HiPIP's (Z_1) obtained from the Watkins electrostatic treatment (Table I) yielded a sign for the charge at the interaction site for all HiPIP's that is the same as the protein net charge, although the magnitudes are considerably smaller. This is in contrast to the above-mentioned cytochrome–FMN system (Meyer et al., 1984), in which active-site charge signs opposite to the protein net charge were observed in some cases for proteins with highly asymmetric charge distributions. For the HiPIP's, the proposed site for electron transfer (Mizrahi & Cusanovich, 1980), which is where the Fe–S cluster is nearest to the protein surface, has been found for a number of reductants to be weakly charged and primarily hydrophobic (Mizhari et al., 1980; Mizrahi & Cusanovich, 1980; Aprahamian & Feinberg, 1981). In the present work, both the sign and the magnitude of the ionic strength effects on the kinetics for the FMN, as well as for the flavodoxin (see below), reactions with HiPIP suggest a model in which the charges are more or less uniformly distributed over the HiPIP protein surface and in which there are both localized and long-range interactions. This is consistent with the structural information available for HiPIP, as shown in Figure 2 where an electrostatic field calculated at the 2-kT level is overlaid on the *Chromatium vinosum* HiPIP backbone structure. The field

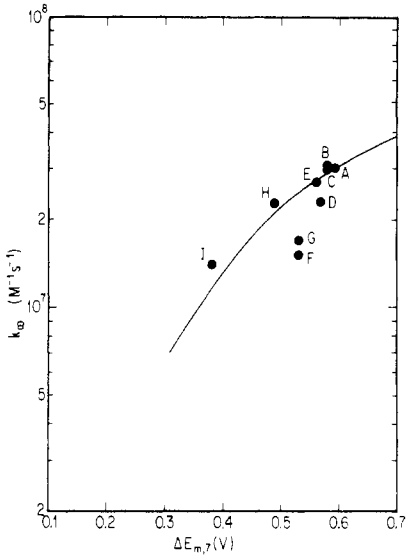

FIGURE 3: Semilog plot of the apparent second-order rate constants extrapolated to infinite ionic strength (k_∞) vs. the difference in redox potential between the reactants (ΔE) for FMN semiquinone oxidation by HiPIP. (Solid line) Plot of Marcus exponential equation with ν_{ET} = 6.0 × 10^7 M^{-1} and $\Delta G^*(0)$ = 3.7 kcal/mol. Labels as in Figure 1.

was calculated by using the method of Matthew & Richards (1982) with the dashed lines indicating regions of negative charge and the solid lines (excluding the protein backbone) reflecting regions of positive charge. As can be seen, no strongly charged regions exist. This is in sharp contrast to mitochondrial cytochrome *c* as well as flavodoxin (Matthew et al., 1983). The most important of the short-range electrostatic interactions is probably due to the single negative charge on the iron–sulfur cluster itself. For those HiPIP's with a net positive charge, viz., *Rhodopseudomonas gelatinosa* and *Rhodosprillum tenue*, the longer range interactions are apparently sufficient to overcome the localized negative charge on the cluster, and the ionic strength effect is exceedingly small. In the net negatively charged proteins, on the other hand, the longer range interactions apparently reinforce the localized charge effect in some instances.

Assuming that histidine has a p*K* value of 6, *C. vinosum*, *Chromatium gracile*, and *Thiocapsa pfennigii* HiPIP's would have net charges of 4–, 6–, and 8– (cf. Table I). However, the slopes of the $k(I)$ vs. ionic strength plots (Figure 1) are essentially identical for these three proteins. Thus, these HiPIP's appear to have similar interaction domain charges (~1.0–; Table I). On the basis of the relative numbers of histidine residues in these proteins, one might be able to explain the ionic strength effects in terms of net protein charges if the histidines had unusually high ionization constants, i.e., p*K*'s near 8. However, the only ionization constant which has been measured, that of *C. vinosum* His-42, has a p*K* of 6.7 (Nettesheim et al., 1983). We thus conclude that local charges play a significant role in the ionic strength effects.

The k_∞ values (i.e., the rate constants for conditions in which all charge effects are presumably cancelled by screening) obtained from the fits in Figure 1 (Table I) were used to examine the dependence of the kinetics on the redox potential difference for the reaction (Figure 3). As can be seen, a correlation between k_∞ and redox potential clearly exists, as was observed in our previous work (Meyer et al., 1984; Tollin et al., 1984). The general trend of the data points can be represented by a curve generated from the Marcus (1968) equation, with the specific curve shown in Figure 3 obtained by adjusting the values of the parameters ν_{ET} and $\Delta G^*(0)$ to include as many of the data points as possible (see legend to Figure 3). A similar fit can be obtained by using the Hopfield equation (1974) (not shown). There is appreciable scatter in the data about the theoretical curve, which may result from the effect of factors other than electrostatics and redox potential, e.g., steric interactions. In the case of the reactions of FMN and flavodoxin semiquinone with *c*-type cytochromes (Meyer et al., 1984; Tollin et al., 1984), it was found that similar deviations from the theoretical curves could in fact be adequately explained (for those cases in which three-dimensional structures were available) in terms of steric differences at the site of electron transfer. Unfortunately, for the HiPIP series, only one structure has been determined (*C. vinosum*). Elucidation of additional HiPIP three-dimensional structures should provide the opportunity to test this possibility.

The $\Delta G^*(0)$ value (which reflects the structural rearrangements which must occur prior to electron transfer) for the Marcus equation (3.7 kcal mol^{-1}) is the same as previously found for other HiPIP–free flavosemiquinone oxidation reactions (Meyer et al., 1983) and is much smaller than the flavodoxin value (see below). The ν_{ET} value (6.0 × 10^7 M^{-1} s^{-1}), which measures the limiting rate constant as ΔE approaches infinity, and thus measures an intrinsic reactivity, is smaller than that previously found (Meyer et al., 1983) for the lumiflavin semiquinone reaction (9.6 × 10^7 M^{-1}). A lower value for FMN relative to lumiflavin was also observed for the *c*-type cytochromes and was interpreted as being due in part to the slightly higher p*K* value for the FMN semiquinone [i.e., less of the intrinsically more reactive anionic flavosemiquinone is present; cf. Przysiecki et al. (1984)] as well as to steric effects from the ribityl phosphate side chain (Meyer et al., 1984). However, the decrease in ν_{ET} (37%) is considerably smaller than that observed for the *c*-type cytochromes (73%; Meyer et al., 1984) and suggests that the phosphate group is exerting a much smaller steric effect in the case of HiPIP reduction.

The electron-transfer reactions between flavodoxin semiquinone and all of the HiPIP's studied were biphasic over the time range available. In general, the rate constant for the slow phase was at least 10 times less than that of the fast phase, so that deconvolution was relatively easy. The fast phase gave linear semilogarithmic plots over 3–4 half-lives and comprised typically 70–80% of the total reaction observed. This was true for all HiPIP concentrations studied, for all ionic strengths, and for each HiPIP source. This is similar to what was found previously for the flavodoxin–cytochrome *c* reaction (Simondsen et al., 1982). In other protein–protein reactions involving HiPIP and *c*-type cytochromes, biphasic kinetics have also been observed; however, the heterogeneity was found to be cytochrome dependent (Mizrahi & Cusanovich, 1980). This suggests, in contrast to an earlier interpretation (Simondson et al., 1982), that the slow reaction observed here may reside with flavodoxin. Further experimentation is required to determine if this is indeed the case. For the present study, only the fast reaction, which represents flavodoxin semiquinone oxidation via electron transfer to oxidized HiPIP (Simondsen et al., 1982), will be discussed further.

Plots of the logarithm of the apparent second-order rate constants vs. the square root of the ionic strength for the reactions of 10 HiPIP's with flavodoxin semiquinone are shown in Figure 4. A comparison with Figure 1 demonstrates that the sign of the charge at the HiPIP interaction site is the same as that for FMN and that the magnitude of V_{ii} is larger for flavodoxin (compare Table I and Table II). As for the HiPIP–FMN semiquinone data, the solid lines were obtained by

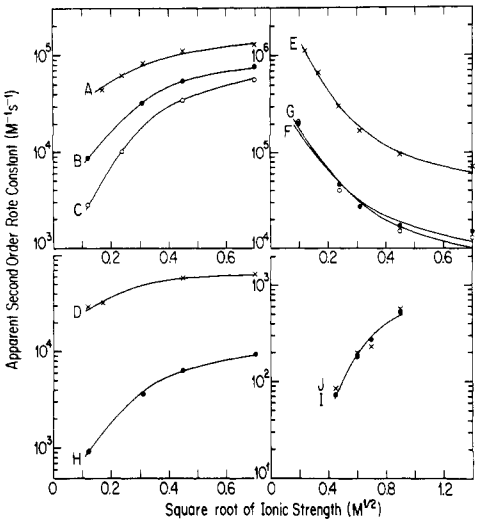

FIGURE 4: Ionic strength dependence of the apparent second-order rate constants for electron transfer from flavodoxin semiquinone to oxidized HiPIP. Solid lines represent theoretical fits of the data to eq 1 (see text for details). Curves for the different HiPIPs labeled as in Table I.

Table II: Effect of Ionic Strength on the Oxidation of Flavodoxin Semiquinone by HiPIP

HiPIP source	V_{ii} (kcal/mol)	ρ (Å)	Z_1[a]	$k_\infty \times 10^5$ (M^{-1} s^{-1})
C. vinosum	+2.62	7.25	−1.0	1.62
C. gracile	+4.20	7.25	−1.6	1.04
T. pfennigii	+5.90	7.25	−2.3	0.88
T. roseopersicina	+1.57	7.25	−0.6	0.71
Rps. gelatinosa	−5.59	7.25	+2.2	0.42
Rsp. tenue 3761	−5.14	7.25	+2.0	0.082
Rsp. tenue 2761	−5.50	7.25	+2.1	0.071
E. vacuolata iso-1	+4.49	7.25	−1.8	0.130
E. vacuolata iso-2	+15.5	7.25	−6.0	0.0087
E. halophila iso-1	+14.3	7.25	−5.6	0.0079

[a] Parameters defined as in footnote *b* of Table I except $Z_2 = -4.0$ and $D_e = 30$; see text for details.

fitting the observed rate constants using eq 1. Table II summarizes the results of these fits. For the analysis, ρ was taken as 7.25 Å, inasmuch as this value yielded excellent fits and is also the same as was used in the flavodoxin–cytochrome *c* study (Tollin et al., 1984). The R_{12} value used was 8.0 Å (as in the HiPIP–FMN semiquinone reaction), and a charge of 4− was used for the flavodoxin interaction domain (Z_2). This latter value was obtained from the computer-modeled flavodoxin–cytochrome *c* complex and is in qualitative agreement with the negative charge observed for flavodoxin semiquinone in reactions with a number of charged oxidants (Simondsen et al., 1982; Tollin et al., 1984). A value of 30 for D_e was used rather than the D_e of 10 which was previously used for the flavodoxin–cytochrome system. This was based upon the fact that the electrostatic fields in the HiPIP's are apparently more diffuse than in the *c*-type cytochromes, so that one would expect weaker protein–protein interactions and hence less exclusion of water from within the interaction domain (Tollin et al., 1984). As can be seen, the calculated Z_1 values range from slightly smaller to substantially greater for flavodoxin as compared to FMN. This is in contrast to the cytochrome–flavodoxin reactions where Z_1 was uniformly larger than that found for FMN, presumably due to the larger interaction domain for the protein–protein system (Tollin et al., 1984). In the absence of more HiPIP structures, it is difficult to interpret the apparently uncorrelated Z_1 values between FMN and flavodoxin. Since the HiPIP's are considerably

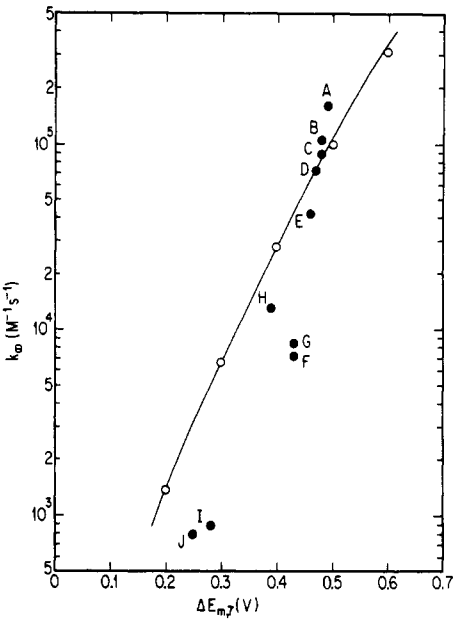

FIGURE 5: Semilog plot of the second-order rate constants extrapolated to infinite ionic strength (k_∞) vs. the difference in redox potential between the reactants (ΔE) for the oxidation of flavodoxin semiquinone by HiPIP. (Solid line) Plot of Marcus exponential equation with $\nu_{ET} = 2.8 \times 10^9$ M^{-1} s^{-1} and $\Delta G^*(0) = 10.7$ kcal/mol; (open circles) plot of Hopfield tunneling equation with $R_p = 15$ Å, $r = 8.0$ Å, $N_a = 8$, $N_b = 12$, and $\Delta_{a+b} = 1.3$ eV where R_p is the protein radius, r is the distance of closest approach between the redox centers, N_a and N_b are the number of atoms over which the initial and final wave functions are distributed for the flavin and HiPIP, respectively, and Δ_{a+b} is the vibronic coupling factor. Labels as in Figure 4.

smaller than flavodoxin, a relatively large proportion of their surface area should be at the site of interaction. Moreover, there are a number of deletions in the smaller HiPIP's. Thus, it is possible that both D_e and R_{12} could vary between different HiPIP's and further complicate the analysis.

The k_∞ values obtained from the fits in Figure 4 (Table II) were used to examine the dependence of the kinetics on the redox potential difference for the reaction (Figure 5), as was done for the HiPIP–FMN semiquinone data. As can be seen, a correlation between rate constant and ΔE exists, and again some deviations from a single theoretical line occur. In this case, curves for both the Marcus (1968) equation (solid line) and the Hopfield (1974) equation (open circles) are shown and are identical. Attempts to obtain steeper curves (which would appear to fit the data better) resulted in physically unreasonable values for the parameters (i.e., ν_{ET} values $>10^{20}$ M^{-1} s^{-1} for the Marcus equation and $r < 4.5$ Å for the Hopfield equation).

The interaction with flavodoxin semiquinone appears to amplify the difference between the k_∞ values and the theoretical curve in the case of the two *Rsp. tenue* HiPIP's, as compared to the FMN semiquinone reaction. In addition, the *Ectothiorhodospira vacuolata* iso-2 and *Ectothiorhodospira halophila* HiPIP's also appear to be significantly less reactive toward flavodoxin semiquinone. Thus, the k_∞ values for the *tenue* HiPIP's are approximately 2-fold less than expected from the Marcus curve for the FMN semiquinone reaction and approximately 5-fold less than expected for the flavodoxin–semiquinone reaction. This type of amplification effect was also observed with the *c*-type cytochromes (Tollin et al., 1984), and the larger and more constrained interaction domain for the flavodoxin reaction was suggested to be the cause (see below for further discussion). With FMN, the *E. vacuolata* protein apparently behaved normally (the *E. halophila* HiPIP

reaction was too slow to measure). A detailed interpretation of these results in terms of surface topology of the various HiPIP's will have to await additional structural data.

Although in the case of the cytochromes a strong interaction mechanism (i.e., that described by the Marcus equation) is possible because of the heme exposure, the lack of any apparent solvent-exposed atoms for the 4Fe–4S cluster in HiPIP makes such a mechanism harder to visualize and suggests that tunneling may be occurring. At present, however, no experimental evidence exists to allow a choice between these two possibilities.

A striking difference between flavodoxin semiquinone oxidation by HiPIP's (Figure 5) and by cytochrome *c* (Tollin et al., 1984), vs. free FMN semiquinone oxidation (Figure 3; Meyer et al., 1984), is the larger dependence of the flavodoxin reactions on ΔE [which is reflected in the larger ν_{ET} and $\Delta G^{\ddagger}(0)$ values for the theoretical fit]. Expressed in another way, the k_{∞} values for *C. vinosum* and *E. vacuolata* HiPIP's differ by ~300-fold for flavodoxin semiquinone oxidation and by only ~3-fold for FMN semiquinone oxidation. This type of result has been previously interpreted (Tollin et al., 1984) in terms of placing the flavosemiquinone (FMN in the present case) into a protein environment which increases its intrinsic reactivity. The larger values for $\Delta G^{\ddagger}(0)$ suggest that more structural rearrangements are required to reach the transition state for flavodoxin semiquinone than for free FMN semiquinone. The HiPIP results are thus consistent with these interpretations.

The effect of electrostatic interactions is, as already mentioned, larger for flavodoxin than for FMN because of the greater charge and the larger interaction domain at the site of electron transfer in flavodoxin. For example, the rate constant value increases ~9-fold for flavodoxin semiquinone oxidation by *C. vinosum* HiPIP vs. ~3-fold for FMN semiquinone oxidation over an ionic strength range of 0.014–0.49 M (the 0.014 M rate constant for FMN semiquinone oxidation was calculated from the parameters in Table I). This can be compared with the rate constants for tuna cytochrome *c* oxidation of FMN and flavodoxin semiquinones which vary by factors of 3 and 100, respectively, over an ionic strength range of 0.058–0.5 M. The larger effect of ionic strength with cytochrome *c* as compared to HiPIP is consistent with the larger electrostatic field near the proposed site of electron transfer [i.e., the exposed heme edge; cf. Tollin et al. (1984)].

The larger magnitudes of the steric, redox potential, and electrostatic effects observed for flavodoxin semiquinone oxidation by cytochromes as compared to those for free FMN have led to the suggestion that these are the principal factors involved in the determination of the biological specificity of electron transfer among redox proteins (Tollin et al., 1984). The similar results of the present study with the HiPIP's provide further support for this concept.

ACKNOWLEDGMENTS

We are grateful to Dr. Patricia Weber for calculating the electrostatic field at the surface *C. vinosum* HiPIP shown in Figure 2.

Registry No. FMN semiquinone, 34469-63-1.

REFERENCES

Aprahamian, G., & Feinberg, B. A. (1981) *Biochemistry 20*, 915–919.

Augustin, M. A., Chapman, S. K., Davies, D. M., Watson, A. D., & Sykes, A. G. (1984) *J. Inorg. Biochem. 20*, 281–289.

Bartsch, R. G. (1978) *Methods Enzymol. 53*, 329–340.

Carter, C. W., Jr. (1977) in *Iron–Sulfur Proteins* (Lovenberg, W., Ed.) Vol. 3, pp 157–204, Academic Press, New York.

Carter, C. W., Jr., Kraut, J., Freer, S. T., & Alden, R. A. (1974) *J. Biol. Chem. 249*, 6339–6346.

Cusanovich, M. A., & Tollin, G. (1980) *Biochemistry 19*, 3343–3347.

Geren, L. M., & Millett, F. (1981) *J. Biol. Chem. 256*, 4851–4855.

Hopfield, J. J. (1974) *Proc. Natl. Acad. Sci. U.S.A. 71*, 3640–3644.

Jung, J., & Tollin, G. (1981) *Biochemistry 20*, 5124–5127.

Marcus, R. A. (1968) *J. Phys. Chem. 72*, 891–899.

Matthew, J. B., & Richards, F. M. (1982) *Biochemistry 21*, 4989–4999.

Matthew, J. B., Weber, P. C., Salemme, F. R., & Richards, F. M. (1983) *Nature (London) 301*, 169–171.

Meyer, T. E., Przysiecki, C. T., Watkins, J. A., Bhattacharyya, A., Simondsen, R. P., Cusanovich, M. A., & Tollin, G. (1983) *Proc. Natl. Acad. Sci. U.S.A. 80*, 6440–6744.

Meyer, T. E., Watkins, J. A., Przysiecki, C. T., Tollin, G., & Cusanovich, M. A. (1984) *Biochemistry 23*, 4761–4767.

Mizrahi, I. A., & Cusanovich, M. A. (1980) *Biochemistry 19*, 4733–4737.

Mizrahi, I. A., Meyer, T. E., & Cusanovich, M. A. (1980) *Biochemistry 19*, 4727–4733.

Nagy, J., Knoll, J., Kenney, W. C., & Singer, T. P. (1982) in *Flavins and Flavoproteins* (Massey & Williams, Eds.) pp 573–578, Elsevier/North-Holland, New York.

Nettesheim, D. G., Meyer, T. E., Feinberg, B. A., & Otos, J. O. (1983) *J. Biol. Chem. 258*, 8235–8239.

Przysiecki, C. T., Tollin, G., Meyer, T. E., Staggers, J. E., & Cusanovich, M. A. (1985) *Arch. Biochem. Biophys. 238*, 334–343.

Rees, D. C. (1980) *J. Mol. Biol. 141*, 323–326.

Simondsen, R. P., & Tollin, G. (1983) *Biochemistry 22*, 3008–3016.

Simondsen, R. A., Weber, P. C., Salemme, F. R., & Tollin, G. (1982) *Biochemistry 21*, 6366–6375.

Tedro, S. M., Meyer, T. E., Bartsch, R. G., & Kamen, M. D. (1981) *J. Biol. Chem. 256*, 731–735.

Tollin, G., Cheddar, G., Watkins, J. A., Meyer, T. E., & Cusanovich, M. A. (1984) *Biochemistry 23*, 6345–6349.

Watkins, J. A. (1985) Ph.D. Dissertation, University of Arizona, Tucson, AZ.

Wherland, S., & Gray, H. B. (1976) *Proc. Natl. Acad. Sci. U.S.A. 73*, 2950–2954.

Wherland, S., & Pecht, I. (1978) *Biochemistry 17*, 2585–2591.